33rd Annual International Conference of the IEEE EMBS
Boston, Massachusetts USA, August 30 - September 3, 2011

Fourier Modeling of Porcine Heartbeat and Respiration *In Vivo* for Synchronization of HeartLander Robot Locomotion

Nathan A. Wood, Nicholas A. Patronik, Marco A. Zenati, and Cameron N. Riviere

Abstract— **HeartLander is a small mobile robot which adheres to and navigates over the surface of the heart to provide therapies in a minimally invasive manner. HeartLander's ability to efficiently operate in this dynamic environment is greatly affected by physiological motion, namely the cardiac and respiration cycles. Synchronization of robot motion with minimal intrapericardial pressure results in safer and more efficient travel. The work presented models the physiological components of motion using Fourier series and estimates their parameters using an Extended Kalman Filter. Using the Fourier series parameters, estimates of physiological phase values are calculated to be used for step synchronization. The proposed methods are demonstrated on data from a HeartLander animal study for four locations on the heart. Mean respiration phase estimates are shown to be within 5% of the true respiration phases, while mean cardiac phase estimates are shown to have a minimum error of 11%.**

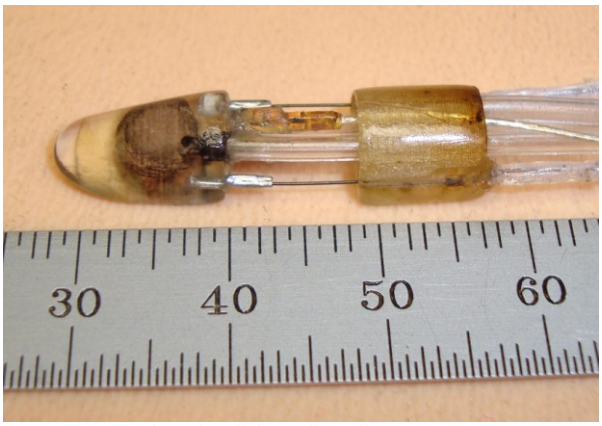

Fig. 1. HeartLander epicardial crawling robot.

I. Introduction

HeartLander is a miniature mobile robot designed to provide therapies to the heart in a minimally invasive manner. The robot adheres to and travels over the epicardial surface of the heart, within the pericardium, by way of a subxiphoid incision in the skin and a small incision to the pericardium.

HeartLander, shown in Fig. 1, crawls using an inchworm-like motion in which flexible drive wires modulate the distance between the tandem body sections. Adhesion to the epicardium is achieved using suction. Motion is generated by extending/retracting the drive wires while suction is alternated appropriately between the body sections. Suction, drive-wire actuation, and 6-DOF magnetic tracking (microBIRD, Ascension Technologies, Burlington, VT) are provided by offboard instrumentation through a flexible tether. This tethered design enables the robot to be extremely small and still produce significant suction and locomotion forces.

Previous animal studies have shown HeartLander's ability to access nearly the entire surface of the heart as well as to navigate precisely to desired targets by suppressing physiological motion in position data using filtering [1]. Although locomotion and targeting was successfully demonstrated in the study, the efficiency of robot motion, defined as the percentage of drive wire motion that resulted in movement of the robot with respect to the heart, was shown to be only 40%. Further work demonstrated that synchronizing the motion of HeartLander with the physiological cycles significantly improved efficiency [2]. This increase in efficiency is due to stepping only when the pressure within the pericardial sac is near its minimum. Synchronization in [2] was achieved by detecting physiological motion events using an accelerometer placed on the surface of the porcine chest.

Recent work has aimed to move from detecting physiological events using external sensors to modeling the motion induced on HeartLander due to respiration and cardiac cycles [3]. This work extends a Kalman Filtering framework for tracking a point of interest on the surface of the heart [4-5] to estimate the position of HeartLander as it navigates over the surface of the beating heart using the available 6-DOF tracking data. The Extended Kalman Filter (EKF) framework models the physiological motions using time-varying Fourier series which enables phase shift estimates to be quickly calculated. Using these techniques, step synchronization was successfully demonstrated on a physiological motion simulator in a laboratory setting [3].

The present work implements the EKF-based physiological motion model on data recorded during previous HeartLander animal studies and investigates the feasibility of detecting physiological phases from the 6-DOF position data. An overview of the EKF estimation framework is presented, as well as the phase value estimation. For a more rigorous description of the EKF

This work was supported in part by the U.S. National Institutes of Health under Grant no. R01 HL078839.

N. A. Wood and C. N. Riviere are with the Robotics Institute, Carnegie Mellon University, Pittsburgh, PA 15213 USA (e-mail: camr@ri.cmu.edu).

N. A. Patronik is with the Atrial Fibrillation Division, St. Jude Medical, New Brighton, MN 55112 USA.

M. A. Zenati is with Harvard Medical School, BHS Department of Cardiothoracic Surgery, West Roxbury, MA 02132 USA.

framework, refer to [3].

II. Methods

A. Physiological Motion Model

The components of robot motion due to the physiological cycles are modeled as separate Fourier series, one for the cardiac motion and one for respiration [5]. The position of the robot, *F*, is then the sum of the respiratory component, *R*, cardiac component, *C*, and a DC offset, *E*. The model of the physiological motion in each direction is given as:

$$F = R + C + E \tag{1}$$

$$R = \sum_{n=1}^{H_r}\left[a_n \sin\left(n\sum_{i=0}^{k}\omega_{r_i}\delta_{t_i}\right) + b_n \cos\left(n\sum_{i=0}^{k}\omega_{r_i}\delta_{t_i}\right)\right] \tag{2}$$

$$C = \sum_{n=1}^{H_c}\left[c_n \sin\left(n\sum_{i=0}^{k}\omega_{c_i}\delta_{t_i}\right) + d_n \cos\left(n\sum_{i=0}^{k}\omega_{c_i}\delta_{t_i}\right)\right], \tag{3}$$

where H_r and H_c are the number of respiratory and cardiac harmonics, ω_r and ω_c are the respiratory and cardiac base frequencies, δt is the time step, i is the time step index, and k is the current time step. The series parameters are a and b for respiratory motion, and c and d for cardiac motion. The DC offset component of the motion model, *E*, is the mean position of the point on the heart to which HeartLander is attached.

The linear velocity of the front foot, U, is the average velocity of the drive wires, v_L and v_R, in the robot/tracker *x*-direction. The motion models of the physiological cycles are constructed in world coordinates requiring the front foot velocity to be transformed into world coordinates. Orientation of the magnetic tracker is represented in quaternion format. Front foot velocity in world coordinates, $\dot{E}$, is then calculated as the front foot velocity in robot coordinates, U, multiplied by the direction of the robot x-axis in world coordinates.

$$U = \frac{v_L + v_R}{2} \tag{4}$$

$$\dot{E} = \begin{bmatrix}\dot{E}_x\\ \dot{E}_y\\ \dot{E}_z\end{bmatrix} = \begin{bmatrix}{q_0}^2+{q_1}^2-{q_2}^2-{q_3}^2\\ 2(q_1q_2+q_0q_3)\\ 2(q_1q_3-q_0q_2)\end{bmatrix}U \tag{5}$$

The state vector of the Kalman Filter is composed of respiratory and cardiac frequencies, ω_r and ω_c, robot location and velocity, E and $\dot{E}$, quaternion orientation, q, and Fourier series parameters for respiration, a and b, and cardiac motion, c and d. The total number of states included depends upon the number of respiratory and cardiac harmonics used. In the prediction step of the EKF, the state at time *k* is estimated as the state at the previous time step for all parameters except for robot location and velocity, E and $\dot{E}$. The estimated robot velocity is calculated as in (5), and the robot position estimate is given by:

$$E_k = E_{k-1} + \dot{E}_{k-1}\delta t_{k-1}. \tag{6}$$

The measurement vector, $y(k)$, used in the update step of the EKF is composed of the position and quaternion from the magnetic tracking system as well as cardiac and respiratory frequencies. Respiration and cardiac frequencies are assumed to be constant and known, and in clinical usage can be measured using an electrocardiogram and ventilator. They are included in the measurement vector so that their values can be updated while the filter is in operation.

$$y(k) = [\omega_r \quad \omega_c \quad x \quad y \quad z \quad q_0 \quad q_1 \quad q_2 \quad q_3]^T \tag{7}$$

B. Phase Estimation and Synchronization

Determination of the phases of the physiological cycles can be calculated using the Fourier series parameters estimated by the EKF. For each harmonic the phase shifts, ϕ_n, can be calculated.

$$\phi_{r_n} = \text{atan2}(-a_n, b_n) \tag{8}$$

$$\phi_{c_n} = \text{atan2}(-c_n, d_n) \tag{9}$$

The physiological phases are described using the notation of Shechter et al. [6]. The respiration cycle is parameterized with expiration occurring in the range -1 to 0 and inspiration in the range from 0 to 1. The cardiac cycle is parameterized with systole occurring in the range from 0 to 0.42 and diastole occurring in the range from 0.42 to 1. In this notation the respiratory and cardiac phase values, θ_r and θ_c, are then estimated using the first-order phase shifts.

$$\theta_r = \frac{mod\left(\sum_{i=0}^{k}\omega_{r_i}\delta_{t_i} + \phi_{r_1}, 2\pi\right)}{\pi} - 1 \tag{10}$$

$$\theta_c = \frac{mod\left(\sum_{i=0}^{k}\omega_{c_i}\delta_{t_i} + \phi_{c_1}, 2\pi\right)}{2\pi} \tag{11}$$

In order for the proposed method of phase value estimation to perform as intended, the directions in which the phase shifts are calculated must be chosen such that they coincide with end-expiration and end-diastole. For example if end-expiration occurs at the maximum tracker value in the x-direction the phase shift is calculated using (8); however, if end-expiration occurs at the minimum tracker value in the x-direction, the proper direction choice is the negative x-direction (-X). This requires the phase shift to be calculated negating a_n and b_n in (8).

III. Results

A. Data

The previously described methods for estimating the phase of physiological cycles were applied to 6-DOF position data logged in a previous animal study. Throughout the animal study the heart was allowed to beat naturally at approximately 78 beats per minute. Breathing was regulated at 0.2 Hz using a ventilator. Access to the heart was achieved through an incision below the sternum, and HeartLander was placed on the epicardium through a second small incision in the pericardium [2].

For the purpose of this study a subset of the data collected in the animal study was used. Four segments of the data were identified in which HeartLander was located on the anterior wall, posterior wall, right lateral wall, and left lateral wall respectively. This subset was selected such that coverage of the heart surface was maximized.

The global reference frame, in which tracker position was reported, was oriented such that the Z-axis was aligned with the anterior-posterior axis, the Y-axis was aligned with the inferior-superior axis, and the X-axis was aligned with the left-right axis, such that the posterior, superior, and rightward directions are positive.

B. True Phase Labeling

In order to evaluate the performance of the presented phase estimation technique, ground truth regarding physiological phase values was derived via offline detection of respiratory and cardiac events in proxy signals. ECG was used to label end-systole events in the cardiac cycle. The Pan-Tompkins detector was used to identify the QRS complex of each heartbeat [7]. The end of diastole corresponds with the end of the QRS complex and a phase value of 0 and 1. Using consecutive end-diastole events, the phase values for each time step within the events are linearly interpolated. For respiration, end-inspiration events were detected using zero-phase-lag filtered data from accelerometers placed on the surface of the porcine chest. End-inspiration corresponds to phase values of -1 and +1. Again, consecutive end-inspiration events were used to interpolate phase values for all time steps within the events.

C. Evaluation

Phase estimation performance was investigated for each of the four robot locations in each principal direction. For each location, the directions which correspond to end-inspiration and end-diastole were identified. At each instant, phase estimation error was calculated by taking the difference of the true phase value and the estimated phase value as a percentage of the total period of the cycle.

Two respiration harmonics and five cardiac harmonics were used in the model in each direction for all trials. Results of a short section of the EKF state estimation while HeartLander is on the left lateral wall of the heart are shown

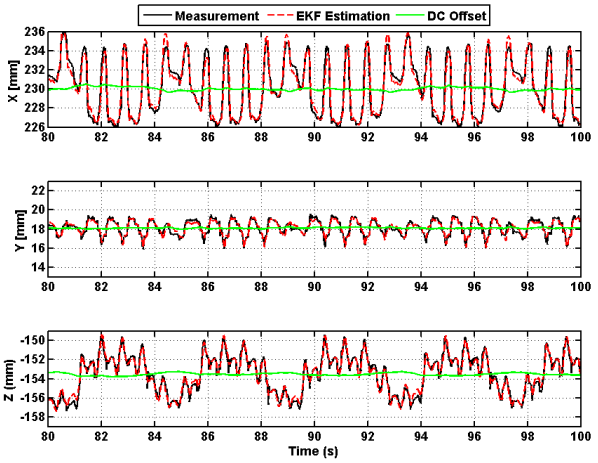

Fig. 2. EKF position estimation of HeartLander while crawling on the left lateral surface of the heart.

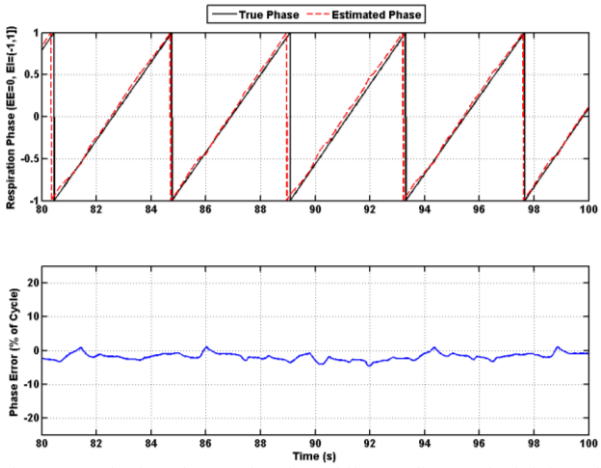

Fig. 3. Respiration phase estimation while crawling on the left lateral surface of the heart. The negative z-direction was used for phase estimation

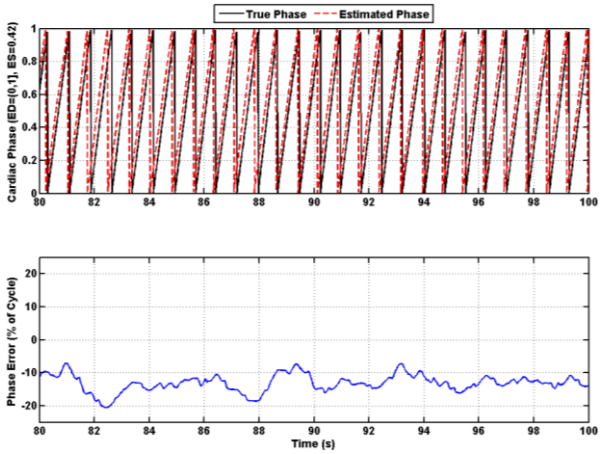

Fig. 4. Cardiac phase estimation while crawling on the left lateral surface of the heart. The negative x-direction was used for phase estimation

TABLE I
RESPIRATION PHASE ESTIMATION RESULTS

Location	Direction	Mean Error [%]	Standard Deviation [%]
Anterior Wall	X	-3.0	4.8
	-Y	-3.7	5.4
	-Z	-3.9	2.0
Posterior Wall	-X	4.8	23.8
	-Y	-4.2	1.0
	-Z	-2.3	0.8
Left Lateral Wall	X	-1.2	1.4
	Y	19.9	12.3
	-Z	-3.1	1.2
Right Lateral Wall	-X	3.7	11.9
	-Y	-0.2	1.8
	-Z	-2.4	1.4

Errors and standard deviations are reported as percentage of a cycle. Negative values indicate that the estimated phase value leads the true phase value.

TABLE II
CARDIAC PHASE ESTIMATION RESULTS

Location	Direction	Mean Error [%]	Standard Deviation [%]
Anterior Wall	-X	-21.9	9.3
	Y	-21.8	5.8
	-Z	-16.2	10.6
Posterior Wall	-X	-10.9	4.5
	-Y	12.5	9.5
	Z	-18.3	6.5
Left Lateral Wall	-X	-13.2	2.8
	-Y	20.0	7.6
	-Z	-20.2	5.1
Right Lateral Wall	X	14.6	3.5
	-Y	22.3	4.9
	-Z	-11.4	4.8

Errors and standard deviations are reported as percentage of a cycle. Negative values indicate that the estimated phase value leads the true phase value.

in Fig. 2. Corresponding phase estimations for respiration and cardiac motion are shown in Figs. 3 and 4, respectively. The estimates of phase were calculated using the negative z-direction (-Z) for respiration and the negative x-direction (-X) for the cardiac phase. Statistics for phase estimation in each direction for each of the four locations are shown in Table I for respiration and Table II for cardiac phase. For respiration, phase estimation was quite accurate, having a mean phase value error of less than 5% for all tests except for the y-direction of the left lateral wall data, where the amplitude of respiratory component of motion was near zero. The amplitude of the respiratory component in the x-direction for the posterior wall test was also very near zero, leading to poor performance and high standard deviation. For each of the four locations on the heart the phase estimation in the negative z-direction (-Z) was less than 4%, with relatively low standard deviation.

Results for cardiac phase estimation were generally less accurate than the respiration phase estimation. The best result achieved occurred for the right lateral wall location in the negative z-direction, which had a mean error of approximately 11%. There was no single global coordinate direction which showed the best performance for all locations.

IV. DISCUSSION

The respiration phase estimation method presented performed well on the animal model data. The respiratory component of motion is slower and more regular than the cardiac component, making its estimation more stable. Also, the phase estimation method worked almost equally well for all four locations in the negative z-direction suggesting that the anterior direction be used for respiration phase detection for the entire heart.

The proposed method did not perform as well for predicting the cardiac phase. The cardiac component of motion is more complicated than the respiration signal, and the first order approximation used when calculating the phase values may be an oversimplification. Work is ongoing on the presented methods to provide more accurate estimates of cardiac phase values.

Planned future work includes animal model studies where greater coverage of the surface of the beating heart is achieved. These tests will be used to demonstrate physiological phase estimation in real time, as well as building a dense map of the motion of the heart due to physiological cycles. Using this data the best coordinate directions to use for phase estimation may be identified for the entire surface of the heart.

REFERENCES

[1] N. A. Patronik, T. Ota, M. A. Zenati, and C. N. Riviere, "A miniature mobile robot for navigation and positioning on the beating heart," *IEEE Trans. Robotics*, vol. 25, pp. 1109-1124, Jan. 2009.

[2] N. A. Patronik, T. Ota, M. A. Zenati, and C. N. Riviere, "Synchronization of epicardial crawling robot with heartbeat and respiration for improved safety and efficiency of locomotion," *Int. J. Med. Robot. Comput. Assist. Surg.,* submitted.

[3] N. A. Wood, D. Moral del Agua, M. A. Zenati, and C. N. Riviere, "Position estimation of an epicardial crawling robot on the beating heart by modeling of physiological motion," *IEEE/RSJ Int. Conf. on Intelligent Robots and Systems*, 2011, submitted.

[4] R. Richa, A. P. L. Bó, and P. Poignet, "Motion prediction for tracking the beating heart," *30th Annu. Int. Conf. IEEE Engineering in Medicine and Biology Society*, 2008, p. 3261–3264.

[5] R. Richa, A. P. L. Bó, and P. Poignet, "Beating heart motion prediction for robust visual tracking," *IEEE Int. Conf. on Robotics and Automation*, 2010, pp. 4579-4584.

[6] G. Shechter, J. R. Resar, and E. R. McVeigh, "Displacement and velocity of the coronary arteries: cardiac and respiratory motion," *IEEE Trans. Med. Imaging*, vol. 25, pp. 369-375, 2006.

[7] J. Pan and W. J. Tompkins, "A real-time QRS detection algorithm," *IEEE Trans. Biomed. Eng.*, vol. 32, p. 230–236, Mar. 1985.